

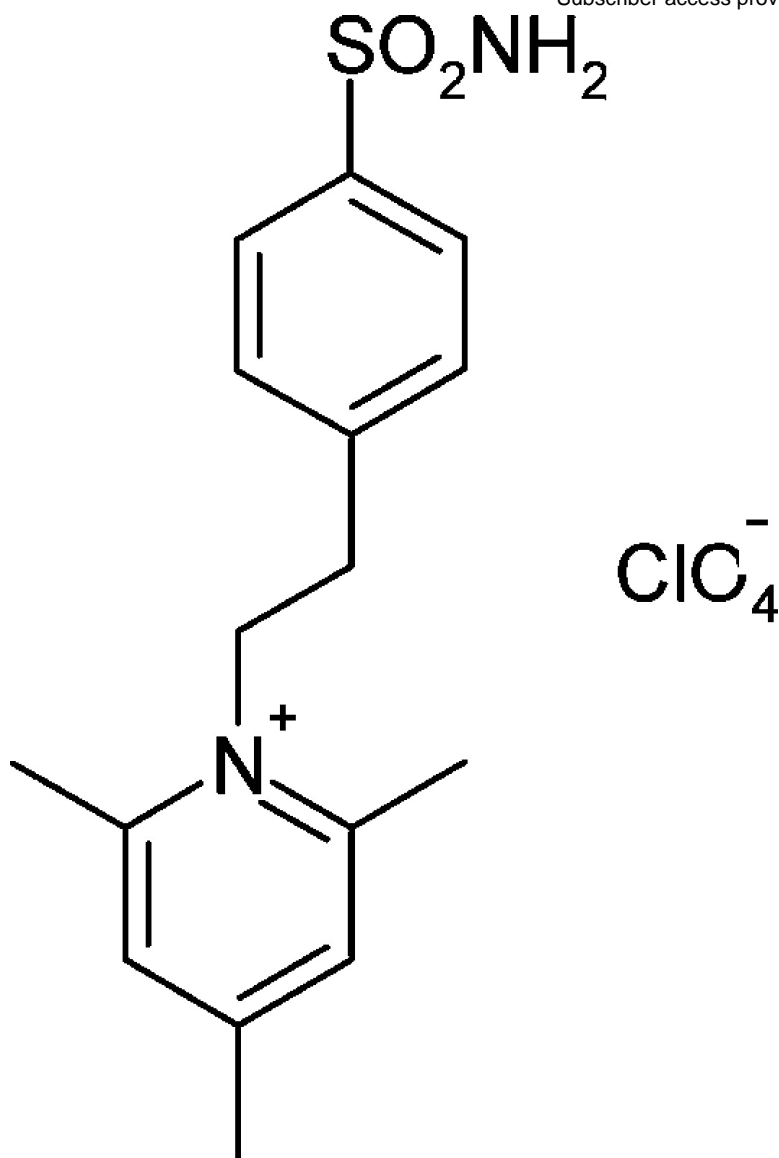
Carbonic Anhydrase Inhibitors: Stacking with Phe131 Determines Active Site Binding Region of Inhibitors As Exemplified by the X-ray Crystal Structure of a Membrane-Impermeant Antitumor Sulfonamide Complexed with Isozyme II

Valeria Menchise, Giuseppina De Simone, Vincenzo Alterio, Anna Di Fiore, Carlo Pedone, Andrea Scozzafava, and Claudiu T. Supuran

J. Med. Chem., **2005**, 48 (18), 5721-5727 • DOI: 10.1021/jm050333c • Publication Date (Web): 06 August 2005

Downloaded from <http://pubs.acs.org> on March 28, 2009





More About This Article

Additional resources and features associated with this article are available within the HTML version:

- Supporting Information
- Links to the 6 articles that cite this article, as of the time of this article download
- Access to high resolution figures
- Links to articles and content related to this article
- Copyright permission to reproduce figures and/or text from this article

Journal of
Medicinal Chemistry

Subscriber access provided by American Chemical Society

[View the Full Text HTML](#)



ACS Publications
High quality. High impact.

Journal of Medicinal Chemistry is published by the American Chemical Society, 1155
Sixteenth Street N.W., Washington, DC 20036

Carbonic Anhydrase Inhibitors: Stacking with Phe131 Determines Active Site Binding Region of Inhibitors As Exemplified by the X-ray Crystal Structure of a Membrane-Impermeant Antitumor Sulfonamide Complexed with Isozyme II

Valeria Menchise,^{†,‡} Giuseppina De Simone,^{*,†} Vincenzo Alterio,[†] Anna Di Fiore,[†] Carlo Pedone,^{†,§} Andrea Scozzafava,^{||} and Claudiu T. Supuran^{*,||}

Istituto di Biostrutture e Bioimmagini-CNR, via Mezzocannone 16, 80134 Naples, Italy, Bioindustry Park del Canavese Spa, Via Ribes 5, 10010 Colletterto Giacosa (Torino), Italy, Dipartimento delle Scienze Biologiche-Sezione Biostrutture, University of Naples "Federico II", via Mezzocannone 16, 80134 Naples, Italy, and Università degli Studi di Firenze, Polo Scientifico, Laboratorio di Chimica Bioinorganica, Rm. 188, Via della Lastruccia 3, 50019 Sesto Fiorentino (Florence), Italy

Received April 12, 2005

Structure for the adduct of carbonic anhydrase II with 1-*N*-(4-sulfamoylphenyl-ethyl)-2,4,6-trimethylpyridinium perchlorate, a membrane-impermeant antitumor sulfonamide, is reported. The phenylethyl moiety fills the active site, making van der Waals interactions with side chains of Gln192, Val121, Phe131, Leu198, Thr200. The 2,4,6-trimethylpyridinium functionality is at van der Waals distance from the aliphatic chain of Ile91 being involved in strong offset face-to-face stacking with Phe131. Analyzing X-ray crystal structures of such adducts, two binding modes were observed: some inhibitors bind with their tail within the hydrophobic half of the active site, defined by residues Phe131, Val135, Leu198, Pro202, Leu204. Other derivatives bind with their tail in a different region, pointing toward the hydrophilic half and making strong parallel stacking with Phe131. This interaction orients the inhibitor toward the hydrophilic part of the active site. Impossibility to participate in it leads to its binding within the hydrophobic half. Such findings are relevant for designing better inhibitors targeting isozymes II, IX, and XII, some of which are overexpressed in hypoxic tumors.

Introduction

The carbonic anhydrases (CAs, EC 4.2.1.1)^{1–3} constitute interesting targets for the design of pharmacological agents useful in the treatment or prevention of a variety of disorders such as glaucoma,^{4–7} acid–base disequilibria,⁸ epilepsy^{9,10} and other neuromuscular diseases,¹¹ altitude sickness,¹² edema,¹³ and obesity.^{14,15} A quite new and unexpected application of the CA inhibitors (CAIs) regards their potential use in the management (imaging and treatment) of hypoxic tumors,¹⁶ since at least two CA isozymes, i.e., CA IX and XII, of the 15 presently known in humans are predominantly found in tumor cells and lack (or are present in very limited amount) in normal tissues.^{17–19} The involvement of these enzymes, which catalyze the simplest physiological reaction, CO₂ hydration to bicarbonate and a proton, in many physiological/pathological processes as well as the fact that generally different isoforms of the 15 mentioned above are involved in such particular processes allows for the development of diverse medicinal chemistry applications of their inhibitors.⁷ Thus, as mentioned above, CA IX and XII are the targets for the development of novel antitumor therapies,^{5,20,21} CA II and XII for the development of antiglaucoma drugs,^{5,6} CA Va and CA Vb for the design of new antiobesity

agents,²² and CA VII for the development of anticonvulsant/antiepileptic drugs,¹⁰ whereas nonvertebrate CAs, such as for example the α -CA present in *Plasmodium falciparum*, may lead to novel types of antimalaria drugs,²³ and the β -CAs from *Mycobacterium tuberculosis* may lead to antimycobacterial agents of new generation,²⁴ to cite only the most important isozymes investigated ultimately for drug design purposes.

Most of the potent CAIs investigated up to now are constituted of an aromatic/heterocyclic sulfonamide⁷ or sulfamate¹⁵ scaffold, to which tails that induce water solubility (or other desired physicochemical properties) are attached. Compounds incorporating other zinc-binding groups have also been investigated.³

These derivatives directly bind by means of the deprotonated sulfonamide/sulfamate moiety to the catalytically critical Zn(II) ion of the enzyme active site, also participating in a multitude of polar and hydrophobic interactions with amino acid residues of the cavity. Typically, clinically used sulfonamide/sulfamate CAIs show potencies in the low nanomolar range against the physiologically relevant isozymes, such as CA I, II, V, and IX.^{7,15} X-ray crystal structures are available for many adducts of pharmacologically relevant inhibitors mainly with isozymes I, II, and IV.^{25–38} Among such compounds recently investigated in some detail by this group are the topically acting antiglaucoma derivatives **1–3**,^{30,31,33} the sulfamate EMATE **4**, also acting as steroid sulfatase inhibitor,³⁶ topiramate **5**, an antiepileptic widely used clinically,³³ the antitumor drug indisulam (E7070) **6** (in phase II clinical trials),³⁷ the antipsychotic sulpiride **7**,³⁵ the COX-2 selective inhibitor

* Correspondence authors. Phone: +39-081-2534579; Fax: +39-081-2536642; E-mail: gmg@chemistry.unina.it (GDS) or Phone: +39-055-4573005; Fax: +39-055-4573385; E-mail: claudiu.supuran@unifi.it (CTS).

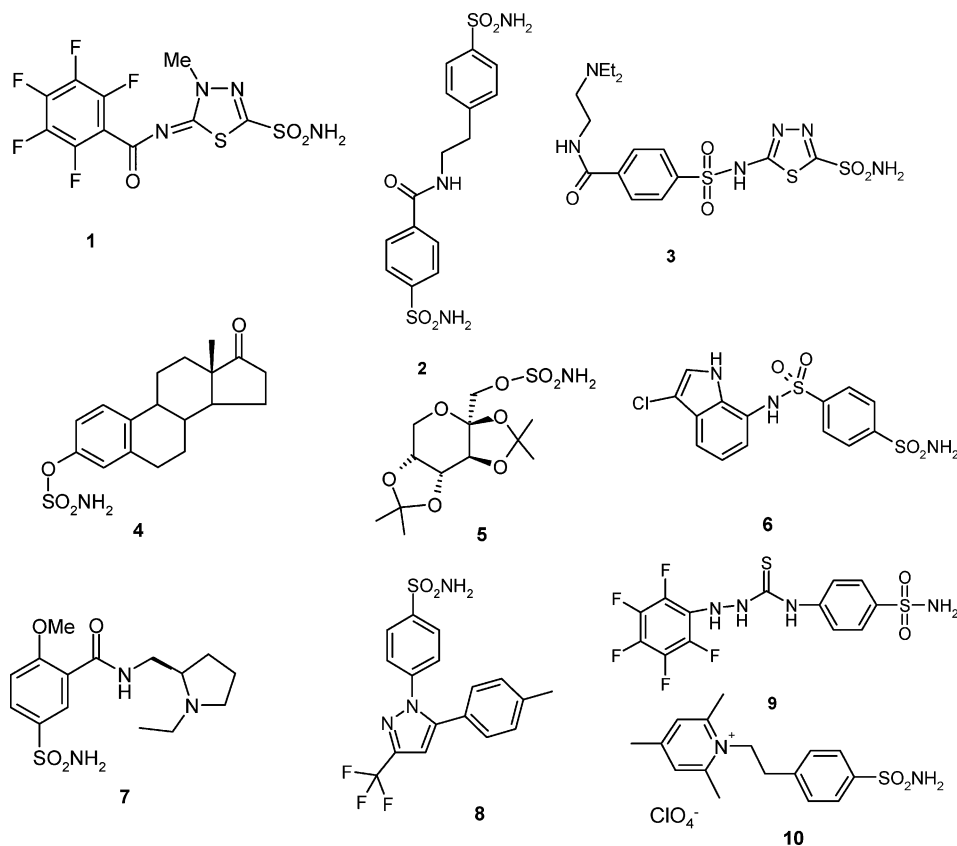
[†] Istituto di Biostrutture e Bioimmagini-CNR.

[‡] Bioindustry Park del Canavese Spa.

[§] University of Naples "Federico II".

^{||} Università degli Studi di Firenze.

Chart 1



celecoxib **8**,³⁸ or the fluorine-containing thiourea **9** also showing good inhibition of the tumor-associated isozyme IX (Chart 1).³⁰ For all these compounds, the X-ray structures in complexes with the physiologically most relevant isozyme, CA II, have been reported at a good resolution (between 1.50 and 2.10 Å) providing important information on the binding modes of these molecules within the enzyme active. In particular, the aromatic/heteroaromatic sulfonamide/sulfamate moiety of all these inhibitors occupies the same position within the hCA II active site, making several van der Waals interactions with the side chains of Gln92, Val121, Phe131, Leu198, and Thr200, in addition to the Zn(II) coordination by means of the sulfonamide/sulfamate nitrogen atom, and participation of the zinc anchor moiety to a network of hydrogen bonds involving the gate-keeper²⁵ residues Thr199 and Glu106. In contrast, two different orientations of the tails used to functionalize these molecules may occur within the enzyme active site: (i) the tails of some inhibitors, such as **2**, **3**, **4**, and **9**, bind within the hydrophobic half of the CA II active site,^{25–27} making favorable and extensive van der Waals interactions with amino acid residues present there (such as Phe131, Val135, Leu198, Pro202, Leu204); (ii) the tails of some other derivatives, such as **1**, **6**, and **7**, present a different orientation, pointing toward the hydrophilic half of the CA II active site defined by residues Asn62, His64, Asn67, and Gln92 and making a strong parallel stacking interaction with Phe131.^{30–38} A third type of binding has been observed for topiramate **5** and celecoxib **8**, as these compounds practically completely fill the entire CA II active site, due to their quite bulky scaffold,³³ but no detailed discussion will be made here on this kind of molecules. Thus, an

important question has arisen during these studies: what are the factors that influence the orientation of an inhibitor when bound to the enzyme active site toward the hydrophobic or hydrophilic part of it? This question is particularly relevant for the design of isozyme-selective CAIs, mainly targeting the cancer-associated isozymes CA IX and XII, which possess several different amino acid residues as compared to CA II just among the ones involved in the binding of inhibitors, such as for example 131 (which is Phe in CA II, Val in CA IX, and Ala in CA XII).³⁹ Here we report the X-ray crystal structure of the adduct of a positively charged, membrane-impermeant sulfonamide^{39–43} CAI, 1-*N*-(4-sulfamoylphenyl-ethyl)-2,4,6-trimethylpyridinium perchlorate **10**, with the human isozyme hCA II. This structure may shed some light both in understanding the binding mode of inhibitors within the CA II active site as well as for the design of better, isozyme-selective compounds targeting the tumor-associated isozyme CA IX, since **10** has recently been shown to diminish *in vitro* the acidification of hypoxic tumors overexpressing this isozyme and may thus constitute an interesting lead for designing antitumor sulfonamides with enhanced activity.¹⁶

Results and Discussion

Chemistry and CA inhibition. The positively charged sulfonamide **10** has been prepared by using pyrylium salts chemistry as reported earlier.^{39,44,45} Inhibition data with derivatives **1–10** against the physiologically relevant isozymes hCA II and hCA IX are shown in Table 1.⁴⁶

It has previously been shown by our group that the only approach for achieving membrane impermeability

Table 1. HCA II and IX Inhibition Data with Compounds 1–10

compound	K_i^a (nM)	
	hCA II ^b	hCA IX ^c
1	1.5	29
2	5.0	18
3	1.4	16
4	10	30
5	5.0	58
6	15	24
7	40	31
8	21	16
9	19	15
10	21	14

^a Mean value from three different determinations (errors were in the range of $\pm 5\%$ of the reported values). ^b Human cloned isozyme. ^c Catalytic domain of the human recombinant isozyme.

with low molecular weight compounds is the design of positively charged CAIs, which being permanently charged are restricted to the extracellular space.^{39–45} Tetraalkylammonium-substituted compounds or pyridinium derivatives, of which **10** is a representative, are membrane-impermeant and thus selectively inhibit only CA isozymes present in the extracellular space, such as the tumor-associated isozymes CA IX and XII.^{39,43} In addition, by making use of the versatile chemistry of pyrylium salts,⁴⁴ such pyridinium derivatives may easily be synthesized bearing a varied range of substitution patterns at the pyridinium ring.^{40–45} Indeed, many representatives of such classes have been reported in recent years, showing that such compounds may lead to effective inhibitors of isozymes CA II, IV, and IX.^{40–45} Although isozyme-selective compounds have not been detected, *in vivo* or *ex vivo*, it has been demonstrated that such derivatives inhibit only the extracellular CA isozymes.^{40–45} This was particularly useful for experiments done with the tumor-associated isozyme CA IX: recently it has been demonstrated, by using the pyridinium derivative **10**, that CA IX is involved in acidification of hypoxic tumors, and that this process may be reverted by inhibiting the enzyme.¹⁶ Indeed, as seen from data of Table 1, **10** is a potent CA IX inhibitor, with an inhibition constant of 14 nM, but it also acts as a strong inhibitor of the cytosolic, physiologically relevant isozyme CA II (K_i of 21 nM). However, *in vivo*, due to the membrane impermeability of **10**, it is probable that the selective inhibition of the membrane-associated isozymes is achieved, without appreciable inhibition of the cytosolic isozyme CA II. This has previously been demonstrated in several models by us, both for *in vivo* as well as *ex vivo* experiments^{40–43} and would confer a restricted number of side effects to potential drugs of this type. Indeed, in tumor cell cultures, compound **10** appreciably inhibited the tumor acidification produced by CA IX, and preliminary *in vivo* data show it to possess the same type of effect *in vivo* after ip administration in rats (unpublished results from this laboratory). Due to the salt-like character and membrane impermeability of this compound, it is improbable that it would be administered *per os*, and the parenteral administration would be necessary, similarly to that of other antitumor drugs, such as E7070 **6**.^{16,37}

Data of Table 1 also show that the other sulfonamides/sulfamates discussed here act as effective inhibitors of both isozymes of interest, with inhibition constants in

Table 2. Data Collection and Refinement Statistics of the hCA II–10 Adduct

Data Collection Statistics (20.00–2.00 Å)	
temperature (K)	100
total reflections	96668
unique reflections	16435
completeness (%)	
overall	91.1
outermost data shell	60.1
R_{sym}^a	
overall	0.067
outermost data shell	0.16
mean $I/\sigma(I)$	
overall	16.3
outermost data shell	5.3
Refinement Statistics (20.00–2.00 Å)	
R-factor ^b (%)	20.4
R-free ^b (%)	25.1
rmsd from ideal geometry:	
bond lengths (Å)	0.007
bond angles (deg)	1.85
number of protein atoms	2060
number of water molecules	198
average B factor (Å ²)	17.85

^a $R_{\text{sym}} = \sum |I_i - \langle I \rangle| / \sum I_i$; over all reflections. ^b R-factor = $\sum |F_o - F_c| / \sum F_o$; R-free calculated with 10% of data withheld from refinement.

the range of 1.4–40 nM against hCA II, and 14–58 nM against hCA IX, respectively. Usually hCA II shows a higher affinity for most of these inhibitors as compared to hCA IX, the only exceptions being celecoxib **8**, the thiourea **9**, and the pyridinium derivative **10**, which all act as better hCA IX than hCA II inhibitors. These results may be explained as due to the quite high similarity between active sites of the two isozymes (the X-ray crystal structure of hCA IX was not reported, so that the sequence homology between the two isozymes is being considered in the following discussion). Indeed, the architecture of the two active sites seems to be quite similar, as the catalytically relevant residues involved in Zn(II) coordination (His94, His96, and His119), the gate-keeper residues (Thr199 and Glu106), and the proton shuttle (His64) are identical in the two isozymes.^{26,39} However, some residues involved in inhibitor binding, such as 131, which is Phe in CA II and Val in CA IX, are different and may explain the differences in inhibitor binding reported in Table 1. Such differences may also lead to the design of inhibitors with a certain degree of selectivity for one of these isozymes.⁶

X-ray Crystallography. The binding mode of **10** to hCA II was analyzed by determining the crystallographic structure of the protein–inhibitor complex. Crystals of the adduct were isomorphous with those of the native protein,^{26b} allowing for the determination of the crystallographic structure by difference Fourier techniques. The model was refined using the CNS program⁴⁷ to crystallographic R-factor and R-free values of 0.204 and 0.251, respectively. The statistics for data collection and refinement are shown in Table 2.

The overall quality of the model was high, with 98.6% of the nonglycine residues located in the allowed regions of the Ramachandran plot (data not shown). The analysis of the electron density maps around the catalytic site allowed placement of one inhibitor molecule in the active site of the enzyme. The topology of the inhibitor binding within the active site is shown in Figure 1.

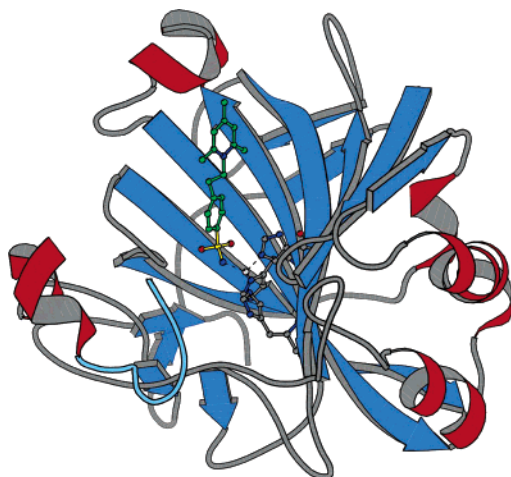


Figure 1. Ribbon diagram of the hCA II–10 complex. The inhibitor, metal coordinating residues H94, H96, H119, and the zinc ion are represented in ball-and-stick.

The structure of the enzyme was not affected by binding of the inhibitor, as shown by the rmsd calculated over all the C α atoms between the hCA II–10 complex and the unbound enzyme^{26b} (rmsd 0.35 Å). Clear electron density was visible for the entire inhibitor (Figure 2) and the protein, except for the first two N-terminal residues. Structural analysis revealed that

the tetrahedral geometry of the Zn²⁺ binding site and the key hydrogen bonds between the sulfonamide moiety of the inhibitor and enzyme active site are all retained with respect to other hCA II–sulfonamide complexes for which X-ray structures have been reported^{7,15} (Figure 3). In particular, the ionized nitrogen atom of the sulfonamide is coordinated to the zinc ion (2.03 Å), displacing the hydroxyl ion/water molecule found in the native enzyme.^{26b} The zinc coordination sphere is completed by the imidazolic nitrogens of His94 (2.02 Å), His96 (1.96 Å), and His119 (2.09 Å). The sulfonamide nitrogen is also involved in a hydrogen bond with the hydroxyl group of Thr199 (2.71 Å), which in turn interacts with the Glu106OE1 atom (2.55 Å). The sulfonamide oxygen O1 accepts a hydrogen bond from the backbone NH moiety of Thr199 (2.79 Å), while O2 is 2.91 Å away from the zinc ion, weakly contributing to its coordination site. The phenylethyl moiety fills the active site channel of the enzyme, making various van der Waals interactions (distance < 4.5 Å) with the side chains of Gln92, Val121, Phe131, Leu198, and Thr200 (Figure 3). The 2,4,6-trimethylpyridinium functionality is at van der Waals distance from the aliphatic chain of Ile91 and is implicated in a strong offset face-to-face stacking interaction with the Phe131 aromatic ring. Its positively charged nitrogen is not involved in any direct binding to the protein, but it is stabilized by several

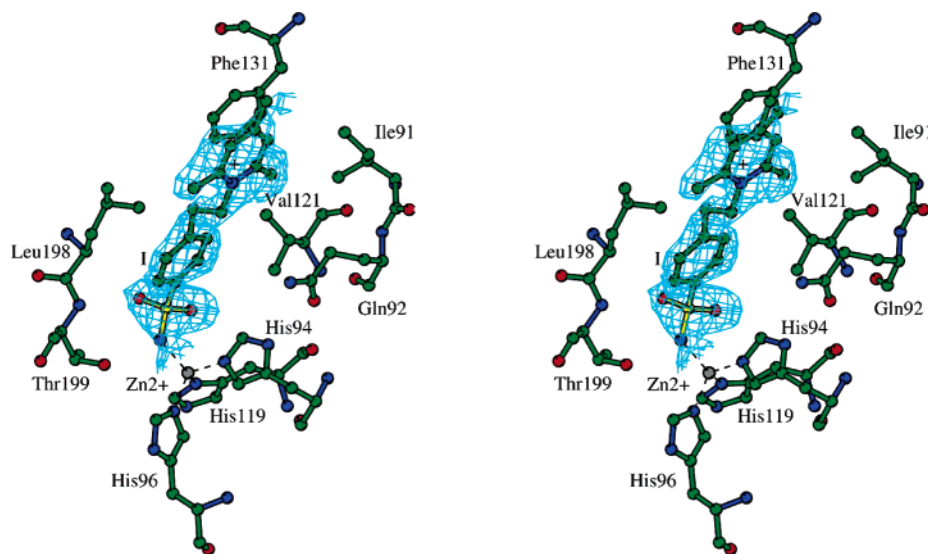


Figure 2. Simulated annealing omit $|2F_o - F_c|$ electron density map, computed at 2.00 Å, and contoured at 1.0 σ for the hCA II–10 complex. The catalytic site region is shown. The inhibitor molecule is identified with the “I” label.

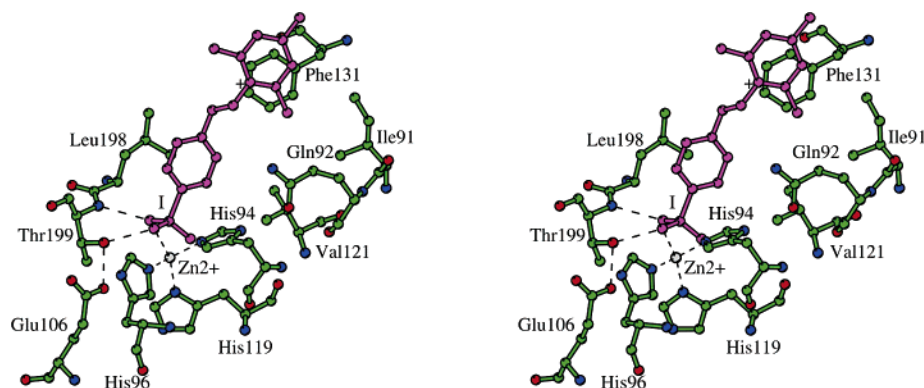


Figure 3. Stereoview of the active site region in the hCA II–10 complex showing the residues participating in recognition of the inhibitor molecule, reported in magenta. Hydrogen bonds and the active site Zn(II) ion coordination are also shown (dotted lines).

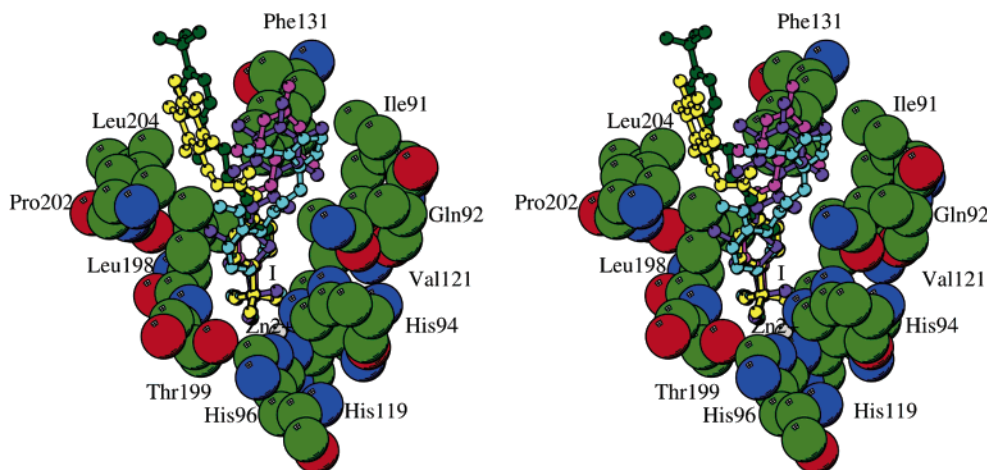


Figure 4. Stereoview of the superimposition of hCA II–inhibitor adducts: **10** is reported in magenta, **1** in purple, **2** in dark-green, **7** in cyan, and **9** in yellow. Amino acid residues critical for inhibitor recognition, the Zn(II) ion, and its three protein ligands are also shown.

dipolar interactions with water molecules present in a solvent channel located in the active site. The peculiar interaction of the pyridinium moiety with Phe131 has been observed only for the indisulam **6** and sulpiride **7**³⁵ benzenesulfonamide inhibitors and the thiadiazoline sulfonamide inhibitor **1** up to now.^{31,34} In fact, in the corresponding enzyme–inhibitor adducts the pentafluorophenyl moiety of **1**, the chloroindole moiety of **6**, and the *N*-ethylpyrrolidine moiety of **7** are also involved in strong parallel stacking interactions with Phe131.^{31,35} In contrast, the tail used to functionalize the other inhibitors discussed here, such as **2**, **3**, **4**, or **9**, were found to be oriented toward the hydrophobic pocket of hCA II, formed by residues Phe131, Val135, Leu198, Pro202, Leu204.^{30,32–34,36–38} The presence of the positive charge on the pyridinium ring of **10** does not appear to be correlated to its orientation, since the neutral tail moieties of compounds **1**, **6**, and **7** are found in the same position within the enzyme active site.^{31,35}

A stereoview of the superimposition of the inhibitors **1**, **2**, **7**, **9**, and **10** when bound to hCA II (Figure 4) helps us to rationalize the different binding modes of CAIs to the enzyme active site. The analysis of this structural superimposition suggests that differences in the spatial arrangement of these compounds are related to the inhibitor length and the possibility to make an offset face-to-face stacking with the phenyl moiety of Phe131. In particular, inhibitors **1**, **7**, and **10** present an optimal structure for establishing this very favorable parallel stacking interaction with Phe131 aromatic moiety described above, while the longer benzenesulfonamide derivatives **2** and **9**^{30,32} are only engaged in weaker hydrophobic interactions in the opposite side of the active site cleft. This behavior is quite well exemplified by the highly different binding of **1** and **9**. These molecules, sharing the same pentafluorophenyl moiety, assume an opposite orientation in the hCA II active site, with the tail of **1** pointing toward the hydrophilic region, and the tail of **9** lying in the hydrophobic half of the active site, probably because of the difference in the length of the molecular fragment connecting the sulfonamide and pentafluorophenyl moieties, and of the possibility only of the C₆F₅ moiety of **1** to participate in a favorable stacking with Phe131.

Conclusions

The X-ray crystal structure for the adduct of hCA II with 1-*N*-(4-sulfamoylphenyl-ethyl)-2,4,6-trimethylpyridinium perchlorate, a membrane-impermeant sulfonamide showing antitumor activity, is reported in this paper. The sulfonamide nitrogen of the inhibitor is coordinated to the zinc ion of the enzyme active site, also being involved in a network of hydrogen bonds with the gate-keeper residues Thr199 and Glu106. The phenylethyl fragment makes various van der Waals interactions with the side chains of Gln92, Val121, Phe131, Leu198, and Thr200. The 2,4,6-trimethylpyridinium functionality is at van der Waals distance from the aliphatic chain of Ile91 and is involved in a strong parallel stacking interaction with the Phe131 aromatic ring. Analysis of several other X-ray crystal structures of hCA II–sulfonamide/sulfamate adducts led to the proposal of two principal binding modes: some inhibitors bind with their tail within the hydrophobic half of the CA II active site, defined by amino acid residues Phe131, Val135, Leu198, Pro202, Leu204. A second group of derivatives, including the positively charged sulfonamide investigated here, bind with their tail in a different region of the active site, pointing toward the hydrophilic half of it and making an offset face-to-face stacking with Phe131. It appears that this last interaction orients the inhibitor toward the hydrophilic part of the active site, whereas impossibility to participate in this stacking leads to the binding of inhibitors within the hydrophobic half. These findings are relevant for the design of better inhibitors targeting isozymes II, IX, and XII, these being overexpressed in hypoxic tumors and correlated with bad disease prognosis.

Experimental Section

Chemistry and CA Inhibition. The positively charged sulfonamide **10** was prepared from 4-aminoethylbenzenesulfonamide (Sigma-Aldrich, Milan, Italy) and 2,4,6-trimethylpyridinium perchlorate⁴⁴ as reported earlier.⁴⁵ Other inhibitors were either commercially available (topiramate, celecoxib, sulpiride) or were prepared as described in the previous work.^{30–38} The recombinant CA isozymes investigated here (hCA II and hCA IX) were obtained from the corresponding cDNAs by the procedure published earlier.^{39,43} Buffers and inorganic reagents were of the highest purity, commercially available compounds from Sigma-Aldrich (Milan, Italy).

An SX.18MV-R Applied Photophysics stopped-flow instrument has been used for assaying the CA-catalyzed CO₂ hydration activity. Phenol red (at a concentration of 0.2 mM) has been used as indicator, working at the absorbance maximum of 557 nm, with 10 mM HEPES (pH 7.5) as buffer, 0.1 M Na₂SO₄ (for maintaining constant the ionic strength), following the CA-catalyzed CO₂ hydration reaction for a period of 10–100 s. The CO₂ concentrations ranged from 1.7 to 17 mM for the determination of the kinetic parameters and inhibition constants. For each inhibitor at least six traces of the initial 5–10% of the reaction have been used for determining the initial velocity. The uncatalyzed rates were determined in the same manner and subtracted from the total observed rates. Stock solutions of inhibitor (1 mM) were prepared in distilled–deionized water with 10–20% (v/v) DMSO (which is not inhibitory at these concentrations), and dilutions up to 0.01 nM were performed thereafter with distilled–deionized water. Inhibitor and enzyme solutions were preincubated together for 15 min at room temperature prior to assay, to allow for the formation of the E–I complex. The inhibition constants were obtained by nonlinear least-squares methods using PRISM 3, from Lineweaver–Burk plots, as reported earlier, and represent the mean from at least three different determinations.⁴⁶

Crystallization, X-ray Data Collection, and Refinement. The hCA II–10 complex was obtained by adding a 10-molar excess of the inhibitor to a 10 mg/mL protein solution in 100 mM Tris–HCl pH 8.5. Crystals of the complex were obtained by the hanging drop vapor diffusion technique at 4.0 °C. The drop consisted of 2 μL of the complex solution and 2 μL of the precipitant solution containing 2.5 M (NH₄)₂SO₄ in 100 mM Tris–HCl (pH 8.2) and 5 mM 4-(hydroxymercurybenzoate) to improve the crystal quality.

Data collection was carried out on a Nonius DIP2030 imaging plate using Cu Kα radiation and one crystal of dimensions 0.3 mm × 0.3 mm × 0.5 mm. The crystal diffracted up to 2.00 Å resolution. Diffracted intensities were processed using the *hkl* crystallographic data reduction package (Denzo/Scalepack).⁴⁸ A total of 96 668 reflections were measured (unit cell parameters: *a* = 42.17 Å, *b* = 41.39 Å, *c* = 72.04 Å, and β = 104.29°) and reduced to 16 435 unique reflections (completeness = 91.1%, R-sym = 6.7% in the 20.00–2.00 Å resolution range).

The structure of the complex was analyzed by difference Fourier techniques, using the PDB file 1CA2^{26b} as a starting model for refinement. Water molecules were removed from the starting model prior to structure factor and phase calculations. The crystallographic R-factor and R-free, calculated in the 20.00–2.00 Å resolution range, based on the starting model coordinates, were 0.308 and 0.350, respectively. Fourier maps calculated with 3F_o – 2F_c and F_o – F_c coefficients showed prominent electron density features in the active site region. After an initial refinement, limited to the enzyme structure (R-factor 0.229 and R-free 0.270), a model for the inhibitor was easily built and introduced into the atomic coordinates set for further refinement, which proceeded to convergence with continuous map inspection and model updates. The refinement was carried out with the program CNS⁴⁷ while model building and map inspections were performed using the program O.⁴⁹ The final crystallographic R-factor and R-free values calculated for the 14 625 observed reflection (in the 20.00–2.00 Å resolution range) were 0.204 and 0.251, respectively. The refined model included 2081 complex atoms, 21 atoms belonging to the inhibitor, and 198 water molecules. The rms deviations from ideal value of bond lengths and bond angles⁵⁰ were 0.007 Å and 1.85°, respectively. The average temperature factor (*B*) for all atoms was 17.85 Å². The stereochemical quality of the model was assessed by Procheck.⁵¹ The most favored and additionally allowed regions of the Ramachandran plot contained 98.6% of the nonglycine residues. The statistics for refinement are summarized in Table 2. Coordinates and structure factors have been deposited in the Brookhaven Protein Data Bank (accession code 1ZE8).

Acknowledgment. This research was financed in part by a grant from the 6th framework of EU (EUROXY project).

References

- Supuran, C. T.; Scozzafava, A.; Conway, J. *Carbonic anhydrase – Its Inhibitors and Activators*; CRC Press: Boca Raton, 2004; p 1–363.
- Scozzafava, A.; Mastrolorenzo, A.; Supuran, C. T. Modulation of carbonic anhydrase activity and its applications in therapy. *Expert Opin. Ther. Pat.* **2004**, *14*, 667–702.
- Pastorekova, S.; Parkkila, S.; Pastorek, J.; Supuran, C. T. Carbonic anhydrases: current state of the art, therapeutic applications and future prospects. *J. Enzyme. Inhib. Med. Chem.* **2004**, *19*, 199–229.
- Marquis, R. E.; Whitson, J. T. Management of glaucoma: focus on pharmacological therapy. *Drugs Aging* **2005**, *22*, 1–21.
- Vullo, D.; Innocenti, A.; Nishimori, I.; Pastorek, J.; Scozzafava, A.; Pastorekova, S.; Supuran, C. T. Carbonic anhydrase inhibitors. Inhibition of the transmembrane isozyme XII with sulfonamides—a new target for the design of antitumor and anti-glaucoma drugs? *Bioorg. Med. Chem. Lett.* **2005**, *15*, 963–9.
- Supuran, C. T.; Casini, A.; Scozzafava, A. Development of sulfonamide carbonic anhydrase inhibitors (CAIs). In *Carbonic anhydrase – Its inhibitors and activators*, Supuran, C. T., Scozzafava, A., Conway, J., Eds., CRC Press: Boca Raton (FL), USA, **2004**, pp 67–148.
- Supuran, C. T.; Scozzafava, A.; Casini, A. Carbonic anhydrase inhibitors. *Med. Res. Rev.* **2003**, *23*, 146–89.
- Loiselle, F. B.; Morgan, P. E.; Alvarez, B. V.; Casey, J. R. Regulation of the human NBC3 Na⁺/HCO₃⁻ cotransporter by carbonic anhydrase II and PKA. *Am. J. Physiol. Cell Physiol.* **2004**, *286*, C1423–33.
- Rivera, C.; Voipio, J.; Kaila, K. Two developmental switches in GABAergic signalling: the K⁺–Cl⁻ cotransporter KCC2 and carbonic anhydrase CAVII. *J. Physiol.* **2005**, *562*, 27–36.
- Vullo, D.; Voipio, J.; Innocenti, A.; Rivera, C.; Ranki, H.; Scozzafava, A.; Kaila, K.; Supuran, C. T. Carbonic anhydrase inhibitors. Inhibition of the human cytosolic isozyme VII with aromatic and heterocyclic sulfonamides. *Bioorg. Med. Chem. Lett.* **2005**, *15*, 971–6.
- Lyons, K. E.; Pahwa, R.; Comella, C. L.; Eisa, M. S.; Elble, R. J.; Fahs, S.; Jankovic, J.; Juncos, J. L.; Koller, W. C.; Ondo, W. G.; Sethi, K. D.; Stern, M. B.; Tanner, C. M.; Tintner, R.; Watts, R. L. Benefits and risks of pharmacological treatments for essential tremor. *Drug Saf.* **2003**, *26*, 461–81.
- Garske, L. A.; Brown, M. G.; Morrison, S. C. Acetazolamide reduces exercise capacity and increases leg fatigue under hypoxic conditions. *J. Appl. Physiol.* **2003**, *94*, 991–6.
- Hori, K.; Ishida, S.; Inoue, M.; Shinoda, K.; Kawashima, S.; Kitamura, S.; Oguchi, Y. Treatment of cystoid macular edema with oral acetazolamide in a patient with best vitelliform macular dystrophy. *Retina* **2004**, *24*, 481–2.
- Supuran, C. T. Carbonic anhydrase inhibitors in the treatment and prophylaxis of obesity. *Expert Opin. Ther. Pat.* **2003**, *13*, 1545–1550.
- Winum, J. Y.; Scozzafava, A.; Montero, J. L.; Supuran, C. T. Sulfamates and their therapeutic potential. *Med. Res. Rev.* **2005**, *25*, 186–228.
- Svastova, E.; Hulikova, A.; Rafajova, M.; Zat'ovicova, M.; Gibadulinova, A.; Casini, A.; Cecchi, A.; Scozzafava, A.; Supuran, C. T.; Pastorek, J.; Pastorekova, S. Hypoxia activates the capacity of tumor-associated carbonic anhydrase IX to acidify extracellular pH. *FEBS Lett.* **2004**, *577*, 439–45.
- Pastorek, J.; Pastorekova, S.; Callebaut, I.; Mornon, J. P.; Zelnik, V.; Opavsky, R.; Zat'ovicova, M.; Liao, S.; Portetelle, D.; Stanbridge, E. J.; et al. Cloning and characterization of MN, a human tumor-associated protein with a domain homologous to carbonic anhydrase and a putative helix-loop-helix DNA binding segment. *Oncogene* **1994**, *9*, 2877–88.
- Rafajova, M.; Zatovicova, M.; Kettmann, R.; Pastorek, J.; Pastorekova, S. Induction by hypoxia combined with low glucose or low bicarbonate and high posttranslational stability upon re-oxygenation contribute to carbonic anhydrase IX expression in cancer cells. *Int. J. Oncol.* **2004**, *24*, 995–1004.
- Ivanov, S.; Liao, S. Y.; Ivanova, A.; Danilkovitch-Miagkova, A.; Tarasova, N.; Weirich, G.; Merrill, M. J.; Proescholdt, M. A.; Oldfield, E. H.; Lee, J.; Zavada, J.; Waheed, A.; Sly, W.; Lerman, M. I.; Stanbridge, E. J. Expression of hypoxia-inducible cell-surface transmembrane carbonic anhydrases in human cancer. *Am. J. Pathol.* **2001**, *158*, 905–19.
- Winum, J. Y.; Pastorekova, S.; Jakubickova, L.; Montero, J. L.; Scozzafava, A.; Pastorek, J.; Vullo, D.; Innocenti, A.; Supuran, C. T. Carbonic anhydrase inhibitors: synthesis and inhibition of cytosolic/tumor-associated carbonic anhydrase isozymes I, II,

- and IX with bis-sulfamates. *Bioorg. Med. Chem. Lett.* **2005**, *15*, 579–84.
- (21) Vullo, D.; Franchi, M.; Gallori, E.; Pastorek, J.; Scozzafava, A.; Pastorekova, S.; Supuran, C. T. Carbonic anhydrase inhibitors: inhibition of the tumor-associated isozyme IX with aromatic and heterocyclic sulfonamides. *Bioorg. Med. Chem. Lett.* **2003**, *13*, 1005–9.
- (22) Vullo, D.; Franchi, M.; Gallori, E.; Antel, J.; Scozzafava, A.; Supuran, C. T. Carbonic anhydrase inhibitors. Inhibition of mitochondrial isozyme V with aromatic and heterocyclic sulfonamides. *J. Med. Chem.* **2004**, *47*, 1272–9.
- (23) Krungkrai, J.; Scozzafava, A.; Reungprapavut, S.; Krungkrai, S. R.; Rattanakaj, R.; Kamchonwongpaisan, S.; Supuran, C. T. Carbonic anhydrase inhibitors. Inhibition of Plasmodium falciparum carbonic anhydrase with aromatic sulfonamides: towards antimalarials with a novel mechanism of action? *Bioorg. Med. Chem.* **2005**, *13*, 483–9.
- (24) Covarrubias Suarez, A.; Larsson, A. M.; Ho Gbom, M.; Lindberg, J.; Bergfors, T.; Bjo Rkelid, C.; Mowbray, S. L.; Unge, T.; Jones, T. A. Structure and function of carbonic anhydrases from mycobacterium tuberculosis. *J. Biol. Chem.* **2005**, *280*, 18782–18789.
- (25) Chakravarty, S.; Kannan, K. K. Drug–protein interactions. Refined structures of three sulfonamide drug complexes of human carbonic anhydrase I enzyme. *J. Mol. Biol.* **1994**, *243*, 298–309.
- (26) (a) Vidgren, J.; Svensson, A.; Liljas, A. Refined structure of the aminobenzolamide complex of human carbonic anhydrase II at 1.9 Å and sulphonamide modelling of bovine carbonic anhydrase III. *Int. J. Biol. Macromol.* **1993**, *15*, 97–100; (b) Eriksson, A. E.; Jones, T. A.; Liljas, A. Refined structure of human carbonic anhydrase II at 2.0 Å resolution. *Proteins Struct. Funct.* **1988**, *4*, 274–282.
- (27) Boriack, P. A.; Christianson, D. W.; Kingery-Wood, J.; Whitesides, G. M. Secondary interactions significantly removed from the sulfonamide binding pocket of carbonic anhydrase II influence inhibitor binding constants. *J. Med. Chem.* **1995**, *38*, 2286–91.
- (28) Stams, T.; Chen, Y.; Boriack-Sjodin, P. A.; Hurt, J. D.; Liao, J.; May, J. A.; Dean, T.; Laipis, P.; Silverman, D. N.; Christianson, D. W. Structures of murine carbonic anhydrase IV and human carbonic anhydrase II complexed with brinzolamide: molecular basis of isozyme-drug discrimination. *Protein Sci.* **1998**, *7*, 556–63.
- (29) Kim, C. Y.; Chandra, P. P.; Jain, A.; Christianson, D. W. Fluoroaromatic-fluoroaromatic interactions between inhibitors bound in the crystal lattice of human carbonic anhydrase II. *J. Am. Chem. Soc.* **2001**, *123*, 9620–7.
- (30) Di Fiore, A.; De Simone, G.; Menchise, V.; Pedone, C.; Casini, A.; Scozzafava, A.; Supuran, C. T. Carbonic anhydrase inhibitors: X-ray crystal structure of a benzenesulfonamide strong CA II and CA IX inhibitor bearing a pentafluorophenylaminothio-ureido tail in complex with isozyme II. *Bioorg. Med. Chem. Lett.* **2005**, *15*, 1937–1942.
- (31) Abbate, F.; Casini, A.; Scozzafava, A.; Supuran, C. T. Carbonic anhydrase inhibitors: X-ray crystallographic structure of the adduct of human isozyme II with the perfluorobenzoyl analogue of methazolamide. Implications for the drug design of fluorinated inhibitors. *J. Enzyme. Inhib. Med. Chem.* **2003**, *18*, 303–8.
- (32) Casini, A.; Abbate, F.; Scozzafava, A.; Supuran, C. T. Carbonic anhydrase inhibitors: X-ray crystallographic structure of the adduct of human isozyme II with a bis-sulfonamide-two heads are better than one? *Bioorg. Med. Chem. Lett.* **2003**, *13*, 2759–63.
- (33) Casini, A.; Antel, J.; Abbate, F.; Scozzafava, A.; David, S.; Waldeck, H.; Schafer, S.; Supuran, C. T. Carbonic anhydrase inhibitors: SAR and X-ray crystallographic study for the interaction of sugar sulfamates/sulfamides with isozymes I, II and IV. *Bioorg. Med. Chem. Lett.* **2003**, *13*, 841–5.
- (34) Abbate, F.; Casini, A.; Scozzafava, A.; Supuran, C. T. Carbonic anhydrase inhibitors: X-ray crystallographic structure of the adduct of human isozyme II with a topically acting antiglaucoma sulfonamide. *Bioorg. Med. Chem. Lett.* **2004**, *14*, 2357–61.
- (35) Abbate, F.; Coetzee, A.; Casini, A.; Ciattini, S.; Scozzafava, A.; Supuran, C. T. Carbonic anhydrase inhibitors: X-ray crystallographic structure of the adduct of human isozyme II with the antipsychotic drug sulpiride. *Bioorg. Med. Chem. Lett.* **2004**, *14*, 337–41.
- (36) Abbate, F.; Winum, J. Y.; Potter, B. V.; Casini, A.; Montero, J. L.; Scozzafava, A.; Supuran, C. T. Carbonic anhydrase inhibitors: X-ray crystallographic structure of the adduct of human isozyme II with EMATE, a dual inhibitor of carbonic anhydrases and steroid sulfatase. *Bioorg. Med. Chem. Lett.* **2004**, *14*, 231–4.
- (37) Abbate, F.; Casini, A.; Owa, T.; Scozzafava, A.; Supuran, C. T. Carbonic anhydrase inhibitors: E7070, a sulfonamide anticancer agent, potently inhibits cytosolic isozymes I and II, and transmembrane, tumor-associated isozyme IX. *Bioorg. Med. Chem. Lett.* **2004**, *14*, 217–23.
- (38) Weber, A.; Casini, A.; Heine, A.; Kuhn, D.; Supuran, C. T.; Scozzafava, A.; Klebe, G. Unexpected nanomolar inhibition of carbonic anhydrase by COX-2-selective celecoxib: new pharmacological opportunities due to related binding site recognition. *J. Med. Chem.* **2004**, *47*, 550–7.
- (39) Pastorekova, S.; Casini, A.; Scozzafava, A.; Vullo, D.; Pastorek, J.; Supuran, C. T. Carbonic anhydrase inhibitors: the first selective, membrane-impermeant inhibitors targeting the tumor-associated isozyme IX. *Bioorg. Med. Chem. Lett.* **2004**, *14*, 869–73.
- (40) Supuran, C. T.; Scozzafava, A.; Ilies, M. A.; Briganti, F. Carbonic anhydrase inhibitors: synthesis of sulfonamides incorporating 2,4,6-trisubstituted-pyridinium-ethylcarboxamido moieties possessing membrane-impermeability and in vivo selectivity for the membrane-bound (CA IV) versus the cytosolic (CA I and CA II) isozymes. *J. Enzyme Inhib.* **2000**, *15*, 381–401.
- (41) Scozzafava, A.; Briganti, F.; Ilies, M. A.; Supuran, C. T. Carbonic anhydrase inhibitors: synthesis of membrane-impermeant low molecular weight sulfonamides possessing in vivo selectivity for the membrane-bound versus cytosolic isozymes. *J. Med. Chem.* **2000**, *43*, 292–300.
- (42) Supuran, C. T.; Scozzafava, A. Benzolamide is not a membrane-impermeant carbonic anhydrase inhibitor. *J. Enzyme. Inhib. Med. Chem.* **2004**, *19*, 269–73.
- (43) Casey, J. R.; Morgan, P. E.; Vullo, D.; Scozzafava, A.; Mastrolorenzo, A.; Supuran, C. T. Carbonic anhydrase inhibitors. Design of selective, membrane-impermeant inhibitors targeting the human tumor-associated isozyme IX. *J. Med. Chem.* **2004**, *47*, 2337–47.
- (44) (a) Balaban, A. T.; Dinculescu, A.; Dorofeenko, G. N.; Fischer, G. W.; Koblik, A. V.; Mezheritskii, V. V.; Schroth, W. *Pyrylium Salts: Syntheses, Reactions and Physical Properties*. In *Advances in Heterocyclic Chemistry*, Katritzky, A. R. (Ed.). Academic Press: New York, 1982; pp. 8–360; (b) Supuran, C. T.; Manole, G.; Dinculescu, A.; Schiketanz, A.; Gheorghiu, M. D.; Puscas, I.; Balaban, A. T. Carbonic anhydrase inhibitors. V: Pyrylium salts in the synthesis of isozyme-specific inhibitors. *J. Pharm. Sci.* **1992**, *81*, 716–9.
- (45) Supuran, C. T.; Scozzafava, A.; Ilies, M. A.; Iorga, B.; Cristea, T.; Briganti, F.; Chiraleu, F.; Banciu, M. D. Carbonic anhydrase inhibitors. Part 53. Synthesis of substituted-pyridinium derivatives of aromatic sulfonamides: The first nonpolymeric membrane-impermeable inhibitors with selectivity for isozyme IV. *Eur. J. Med. Chem.* **1998**, *33*, 577–595.
- (46) Khalifah, R. G. The carbon dioxide hydration activity of carbonic anhydrase. *J. Biol. Chem.* **1971**, *246*, 2561–2573.
- (47) Brünger, A. T.; Adams, P. D.; Clore, G. M.; De Lano, W. L.; Gros, P.; Grosse-Kunstleve, R. W.; Jiang, J. S.; Kuszewski, J.; Nilges, M.; Pannu, N. S.; Read, R. J.; Rice, L. M.; Simonson, T.; Warren, G. L. Crystallography & NMR System: A New Software Suite for Macromolecular Structure Determination. *Acta Crystallogr. Sect. D*, **1998**, *54*, 905–921.
- (48) Otwinowski, Z.; Minor, W. Processing of X-ray diffraction data collected in oscillation mode. *Methods Enzymol.* **1997**, *276*, 307–326.
- (49) Jones, T. A.; Zou, J. Y.; Cowan, S. W.; Kjeldgaard, M. Improved methods for building protein models in electron density maps and the location of errors in these models. *Acta Crystallogr. Sect. A* **1991**, *47*, 110–119.
- (50) Engh, R. A.; Huber, R. Accurate bond and angle parameters for X-ray protein structure refinement *Acta Crystallogr. Sect. A* **1991**, *47*, 392–400.
- (51) Laskowski, R. A.; MacArthur, M. W.; Moss, D. S.; Thornton, J. M. PROCHECK: a program to check the stereochemical quality of protein structures *J. Appl. Crystallogr.* **1993**, *26*, 283–291.

JM050333C